Rapid and efficient detection of single chromophore molecules in aqueous solution

Li-Qiang Li and Lloyd M. Davis

The first experiments on the detection of single fluorescent molecules in a flowing stream of an aqueous solution with high total efficiency are reported. A capillary injection system for sample delivery causes all the dye molecules to pass in a diffusion-broadened stream within a fast-moving sheath flow, through the center of the tightly focused laser excitation beam. Single-molecule detection with a transit time of ~1 ms is accomplished with a high-quantum-efficiency single-photon avalanche diode and a low dead-time time-gating circuit for discrimination of Raman-scattered light from the solvent.

Key words: Single-molecule detection, laser-induced fluorescence, ultrasensitive detection, time-correlated single-photon counting, single-photon avalanche diode.

1. Introduction

Single-molecule detection (SMD) in condensed phases is important for many applications, including high-density optical memory,[1] rapid DNA sequencing,[2] molecular evolutionary biotechnology,[3] environmental studies,[4] and analytical chemistry techniques such as fluorescence immunoassay[5] and capillary electrophoresis.[6] Furthermore, SMD experiments have been used to observe directly statistical differences and stochastic changes in molecular behavior, for fundamental studies of heterogeneous local environments, and for quantum mechanical features such as photon antibunching and quantum jumps.[7]

In recent years considerable progress has been made by the use of a variety of techniques. SMD has now been accomplished within cryogenic solids,[7] on solid surfaces at room temperature by the use of either near-field excitation[8–10] or conventional optics,[11] within electrostatistically suspended glycerol droplets,[12] within a drop of solution attached to the objective of a confocal microscope,[3] and in bulk solution within a flow cell.[13–17]

The experimental technique for SMD in solution within a flow cell involves exciting a picoliter probe region with a rapidly pulsed mode-locked laser, using subnanosecond time-gated single-photon detection to discriminate delayed fluorescence from promptly scattered photons, and identifying the transit of individual molecules by photon burst detection. Recent advancements in SMD within a flow cell have been made possible by the development of a single-photon avalanche diode (SPAD) with >50% quantum efficiency and subnanosecond timing jitter.[17] The increased fluorescence detection efficiency provided by the SPAD has enabled the detection of single chromophore molecules with transit times of ~10 ms.[15,17]

However, in these and all earlier SMD experiments within a flow cell, only a small fraction of the sample molecules pass through the probe region for detection, because the cross-sectional area of the flow cell is considerably larger than that of the probe region. Although previous experiments have claimed detection efficiencies of up to 97%,[15] this is actually obtained by the division of the rate of photon bursts that are above a preselected amplitude by the rate of molecules expected to pass through the central probe region. Molecules that pass near the edges of the Gaussian profile of the laser beam may give detectable photon bursts that compensate for molecules that escape detection because of photodegradation. Furthermore, the molecules that pass near the edges of the laser beam give rise to a monotonic distribution of burst amplitudes without clear distinction from bursts that are due to shot-noise fluctuations in the background. If the threshold is set arbitrarily low and a higher false rate is tolerated, a detection efficiency of over 100% of those expected through the central probe region may be obtained.

The goal of the present work[18] is to develop an experimental system in which almost all sample molecules pass through the center of the probe region

The authors are with the Center for Laser Applications, University of Tennessee Space Institute, Tullahoma, Tennessee 37388.

Received 16 August 1994; revised manuscript received 4 November 1994.

0003-6935/95/183208-10$06.00/0.

so that a high total detection efficiency and a distribution of burst amplitudes with a well-defined peak are obtained. An increase in the rate at which molecules are detected is also sought, so that a large number of molecules may be rapidly counted for analytical applications.

In previous attempts to detect all molecules, hydrodynamic focusing has been used to form a sample stream of diameter as small as ~20 μm, and single molecules of the protein B-phycoerythrin, with the equivalent of 25 Rhodamine 6G (R6G) chromophores, have been detected with transit times of ~0.18 ms. [19] Unfortunately, however, the focused laser beam in these experiments was smaller than the size of the sample stream so that the property of hydrodynamic focusing was never fully used. Efficient detection and a well-defined burst amplitude distribution have been obtained by the use of a hydrodynamically focused stream with a larger probe region, but only with considerably larger and brighter fluorescently stained DNA strands.[20,21] To achieve an adequate signal-to-noise ratio for the detection of weakly fluorescent single chromophore molecules, a smaller probe region and a longer transit time are required. Furthermore, small molecules give faster diffusional spreading and thus a larger stream size with hydrodynamic focusing.

In the present work, the sample is instead injected into a sheath flow through a capillary with a submicrometer hole. Although the sample stream quickly spreads because of diffusion as it passes downstream, almost all molecules will pass through the center of the probe region for detection, provided that the capillary tip is placed directly above the probe region and a sufficiently fast sheath flow is used. To demonstrate that SMD can be achieved at appropriately fast flow speeds, experiments are at first conducted in a simple flow cell, without the sample injection capillary. To detect single chromophore molecules with shorter transit times within the faster sheath flow, an increase in the rate of fluorescence signal is needed. The experimental instrumentation used to achieve SMD with higher fluorescence count rates is described in Section 2.

2. Experimental Setup

Figure 1 shows the experimental setup used for the detection of single molecules in a flow cell. The probe region is excited by a picosecond dye laser (Coherent 702-1) synchronously pumped at 76 MHz by a frequency-doubled mode-locked Nd:YAG laser (Coherent Antares 76-s). For excitation of the commonly used fluorescent tagging molecule, sulforhodamine 101 (S-101), the dye laser is tuned to the peak of the absorption spectrum, at 585 nm. To minimize the Raman and the Rayleigh scatter in the direction of observation, the polarization direction of the excitation beam is rotated so that it is in the plane of the optical table. The excitation beam is focused into the sample cell by the use of the optics discussed in Section 4.

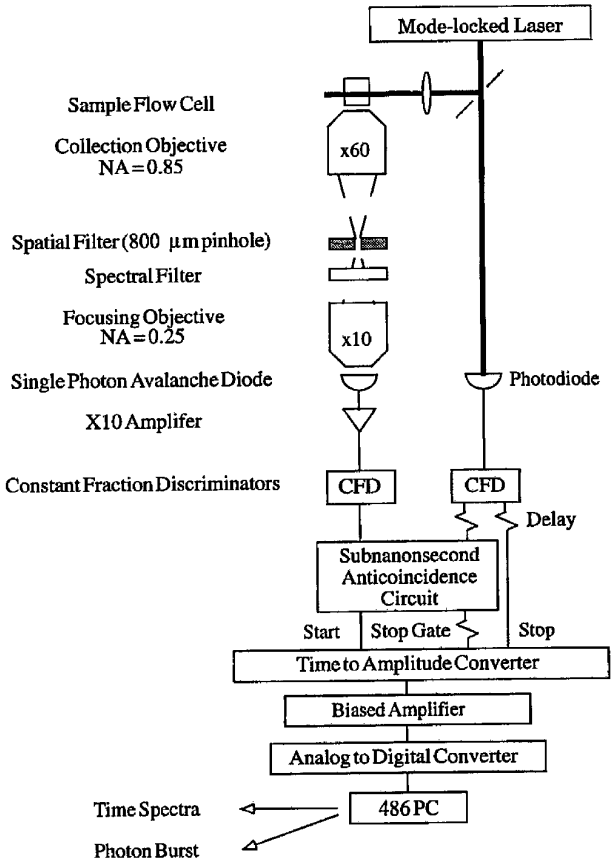

Fig. 1. Experimental setup.

Fluorescence light is collected at right angles with a 60× high numerical aperture (N.A. 0.85) microscope objective (Nikon CF Plan Achromat 79173). A pinhole with a diameter of 800 μm, located at the image plane of the objective, serves as the spatial filter to limit the size of the probe region. Two custom-made six-cavity interference bandpass filters from Omega Optical are used to block the Rayleigh-scattered light from the solvent while passing a large portion of the weak fluorescence signal. Together, the filters provide an optical blocking density at the excitation wavelength of >7.6, i.e., a transmission of $<10^{-7.6}$ and a relatively high throughput from 595 to 665 nm. The integrated transmission of the fluorescence emission spectrum of S-101 is approximately 0.4. Note that the majority of the Raman scattering from the solvent, which is due to the O–H stretching mode that extends from ~3100 to 3700 cm^{-1}, is located at 715–747 nm, outside the transmission range of the filters. The fluorescence and the remaining Raman light that passes through the spectral filters are then focused by a 10× microscope objective (Newport M-10) onto the SPAD.[22]

The SPAD output pulses are amplified by a 20-dB gain, noninverting, 2.2-GHz bandwidth amplifier (B&H Electronics AC2010H) and then conditioned by one channel of a quad constant fraction discriminator (Tennelec TC454). Another channel conditions the output pulses from a fast photodiode (Hewlett-

Packard 5082-4203) for providing the timing signal from the laser excitation pulses. The signals from each of the constant fraction discriminators pass into a locally constructed anticoincidence circuit, which has subnanosecond timing precision and a dead time of ~10 ns. SPAD pulses that are due to promptly scattered Raman light will be approximately coincident with pulses from the excitation channel, and hence most will be blocked.

Instrumentation for time-correlated single-photon counting is then used to provide more precisely adjustable time gating. SPAD pulses that pass the anticoincidence circuit and pulses from the excitation channel are used as the start and stop inputs for the time-to-amplitude converter (TAC) (E.G. & G., Ortec 567), which is operated in reverse mode.[23] As the TAC linearity is best when the conversion time is near the middle of its range, a suitably timed stop pulse is selected by the application of a pulse at the stop gate. Although there is also a start-gate input on the TAC that may be used as an anticoincidence gate, it does not permit subnanosecond timing.

The external anticoincidence circuit, which acts as a temporal prefilter before the TAC, is necessary because the TAC dead time limits the maximum rate of start pulses that can be processed. In this work the count rate is considerably higher than in previous experiments because of the improved detector quantum efficiency, higher numerical aperture collection objective, and moderately sized probe region. The count rate is typically $3 \times 10^5\ s^{-1}$, largely because of Raman photons, while the TAC dead time is ~2.5 μs. Without the temporal prefilter, the TAC would spend most of its time processing Raman photons, and a large portion of the fluorescence photons would be lost.

The fraction of counts that would be lost can be calculated from the mean time between photons, $\bar{u}$. For steady-state random emission, the probability density function of time intervals between successive photons, $p(u)du$, is exponential, i.e.,

$$p(u)du = (1/\bar{u}) \exp(-u/\bar{u})du. \quad (1)$$

The fraction of photons that would arrive during the dead time and be lost is thus

$$\int_0^{t_{dead}} p(u)du = 0.53. \quad (2)$$

Figure 2 shows the time spectrum of the SPAD response after the anticoincidence circuit has been employed. Photon counts concentrated near the peak of the prompt function that are due to Raman scatter have been removed, and the rate of counts at the TAC start is reduced to ~4000 s^{-1}. With the passage of a molecule, the instantaneous count rate increases to $\sim 2 \times 10^4\ s^{-1}$, and the fraction of counts lost because of the TAC dead time is <0.05.

Time gating, with a software-adjustable window, and data processing for photon-burst detection are achieved by one's passing the TAC output pulses

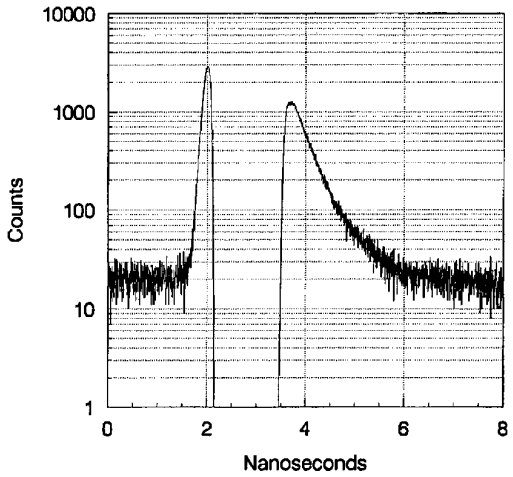

Fig. 2. Time spectrum after the rejection of Raman photons.

through a biased amplifier to a 1-MHz 12-bit analog-to-digital converter (National Instruments EISA-A2000) within a 33-MHz EISA-bus 486 PC. Data-acquisition software, locally written in C, records the number of microseconds between successive TAC pulses, m_i, as well as the amplitude of each pulse, n_i. The values n_i, which correspond to the nanosecond delay between excitation and detection of each photon, are used by the software to construct the time spectrum and select the time-gating window. A stream of numbers, $\bar{m}_i$, corresponding to the number of microseconds between TAC pulses with amplitudes within the window, is formed. The software uses this data array to construct the autocorrelation function and the photon-burst signal.

3. Data Analysis

The time-averaged autocorrelation function has been used as the main criterion for determining whether sufficient sensitivity exists for detecting single molecules.[24] For a signal of amplitude $d(t_i)$, defined at discrete time intervals, the time-averaged autocorrelation function in digital form is given by

$$g(\tau_j) = \sum_i d(t_i)d(t_i + \tau_j), \quad (3)$$

where the sum is taken over the full duration of the experiment. For the data-acquisition system used in this work, at each microsecond time interval, $d(t_i)$ is either 1, if a photon is detected, or 0. The autocorrelation function can thus be rapidly accumulated in real time as the histogram of cumulative delays, $\bar{m}_i$, $\bar{m}_i + \bar{m}_{i-1}$, $\bar{m}_i + \bar{m}_{i-1} + \bar{m}_{i-2}$, . . . , .

The autocorrelation function provides a sensitive test for checking whether the flow system is clean and also is a means for determining the transit time of molecules through the probe region. If no molecules pass through the laser beam and all detected photons occur at random times, then the autocorrelation function consists of a delta function at $\tau_j = 0$ superimposed upon a completely flat background. However,

when molecules pass through the beam and give photon bursts, a broadened peak, with its width proportional to the mean duration of the photon bursts, is formed at the origin.

To determine the proportionality constant, consider a molecule traveling at a constant velocity, v, along the x axis through the center of an elliptical laser beam, with waists ω_x and ω_y and power P. The time-dependent excitation intensity is given by

$$I(t) = (2P/\pi\omega_x\omega_y)\exp(-2v^2t^2/\omega_x^2). \quad (4)$$

For excitation below saturation and no photodegradation, the average fluorescence emission rate, $F(t)$, is proportional to $I(t)$, i.e.,

$$F(t) \propto \exp(-2t^2/\delta_t^2), \quad (5)$$

where $\delta_t = \omega_x/v$ is the half-transit time of the molecule. The autocorrelation of the emission intensity is

$$g(\tau) = F(t)\ F(t) \propto \exp(-\tau^2/\delta_t^2), \quad (6)$$

and thus the standard deviation of the autocorrelation is

$$\sigma_a = \delta_t/\sqrt{2}. \quad (7)$$

Although the autocorrelation function is an indication of single-molecule sensitivity, it cannot be used to indicate the passage of individual molecules. To generate the photon-burst signal, $S(t_i)$, that signifies the passage of individual molecules, it is necessary to process the raw data $\overline{m}_i$.

The simplest data-processing scheme is a simple sliding sum in which, at each time step t_i, all photon counts within a fixed interval are summed to obtain the photon-burst signal as

$$S(t_i) = \sum_{\tau=-\delta_t}^{\delta_t} d(t_i + \tau). \quad (8)$$

Note that the interval over which counts are summed is chosen to be the full-transit time of a molecule, $2\delta_t$. The simple sliding sum corresponds to the signal that would be observed if a multichannel scalar were used. It exhibits a peak whenever the photons are bunched together in a burst.

Apart from the simple sliding sum, other digital filters may be used to enhance the signal. In this experiment, most molecules do not photodegrade, and, on average, the fluorescence emission is expected to be given by expression (5). Hence a digital filter based on a weighted sliding sum, with normalized Gaussian weights directly proportional to expression (5), is adopted, i.e.,

$$S(t_i) = \sum_{\tau=-\delta_t}^{\delta_t} w(\tau)d(t_i + \tau), \quad (9)$$

where

$$w(\tau) = 2\sqrt{2/\pi}\,\exp(-2\tau^2/\delta_t^2). \quad (10)$$

$S(t)$ exhibits a large value whenever the temporal pattern of incoming photons has the characteristic Gaussian profile of a single-molecule fluorescence burst.

4. Flow System and Optical Design

In order to cause all sample molecules to pass through the center of the probe region for detection, the sample is injected into a sheath flow through a capillary with a fine opening at the tip. Molecules exiting from the opening will undergo diffusional spreading as they are carried downstream by the sheath flow. The amount of diffusional spreading in each dimension after a time t is proportional to $\sqrt{2Dt}$, where D is the diffusion coefficient. For small diffusional spreading, the time t that it takes for sample molecules to pass from the opening to the probe region must be small. A small t is obtained by one's placing the capillary tip close to the probe region ($\sim$15 μm) and one's using a fast sheath flow velocity ($\sim 10^{-2}$ ms^{-1}).

Figure 3 shows an intensified CCD image of the sample stream under these conditions obtained with a concentrated dye solution. The injection capillary (Eppendorf Femtotip) has an opening of diameter 0.5 μm ± 0.2 μm and the flow cell consists of glass square-bore tubing (Wilmad WST-8280) of inside dimensions 0.8 mm × 0.8 mm and wall thickness 0.16 mm.

A microscope objective with N.A. = 0.85 is used for efficient light collection from molecules in the fast-flowing stream. The half-angle of the cone of light collection from water is $\theta = \sin^{-1}(\text{N.A.}/1.33) = 40°$, and the collection efficiency is $\sin^2(\theta/2) = 0.12$. The objective has a working distance of 0.41–0.45 mm, which is slightly larger than that required for collecting light from the center of the flow cell (0.4 mm/1.33 + 0.16 mm/1.5). The depth of focus, which is extremely shallow for a high N.A., is $\sim$0.2

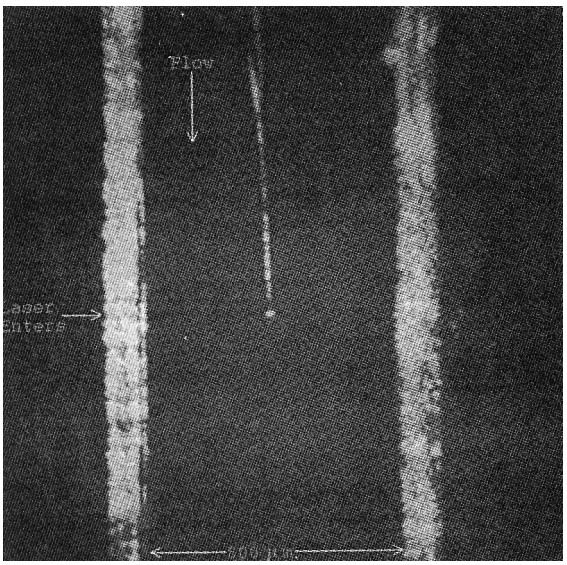

Fig. 3. CCD image of sample stream.

μm. For pure imaging applications, such a shallow depth of focus results in a fuzzy image if the object moves ~0.2 μm toward or away from the objective. However, for light collection, a larger amount of defocusing is tolerable, provided that the spatial filter does not significantly block the enlarged fuzzy image. For the geometry used in this work, the depth of collection (DOC) is estimated to be approximately ±6 μm. This estimate is obtained by imaging laser scatter from a single 0.5-μm-diameter latex microbead suspended in ethylene glycol, through the use of an intensified CCD camera system (Hamamatsu Argus 100).

As indicated in Fig. 4, the size of the probe region is determined by the overlap of the DOC, the tightly focused laser beam, and the field of view of the spatial filter. If all molecules within a sample are to be detected, the sample stream size must be smaller than the DOC and the field of view of the spatial filter. In order to place the capillary tip as close as possible to the center of the laser beam without giving excessive light scatter from the tip, the size of the beam in the flow direction should be small. However, the beam size along the light collection direction should be larger than the DOC to ensure strong excitation throughout the probe region. Therefore an elliptical beam waist that is narrower along the axis of the flow cell is used.

To form the elliptical waist, a pair of cylindrical lenses is used to make a collimated elliptical spot before the focusing lens, as illustrated by L3 and L4 in Fig. 5. The laser beam is then tightly focused into the sample cell by the achromatic doublet lens, L5, with a focal length of 47.6 mm and a clear diameter of 15 mm. As the focused spot size is inversely proportional to the incoming beam diameter, the beam is first expanded to a diameter of ~6.0 mm before it reaches the cylindrical lenses. For this purpose, a 10× microscope objective (f = 14.8 mm) and an achromatic doublet lens (f = 160 mm), indicated by L1 and L2 in Fig. 5, are used.

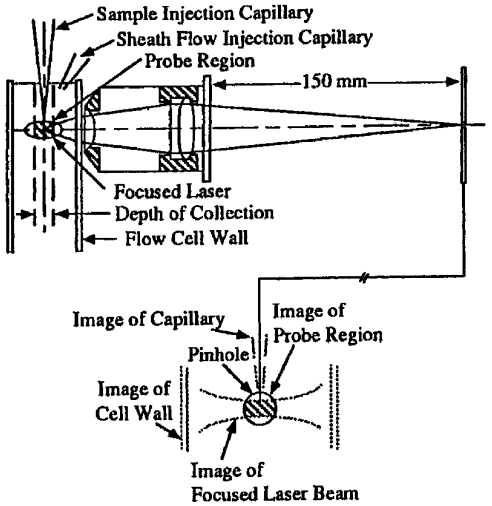

Fig. 4. Probe region and collection optics.

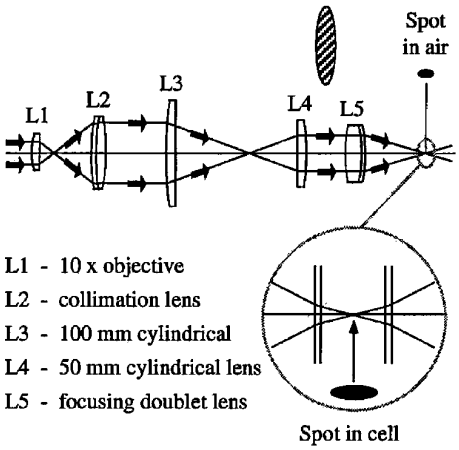

Fig. 5. Focusing optics.

The size of the waist in air is measured as ω_x = 3.6 μm, ω_y = 7.2 μm by a simple method involving gradual eclipsing of the beam by a sharp knife edge. When the flow cell is in place, because of refraction as the beam enters the cell, the divergence angle decreases by a factor of 1.33, which is the ratio of refractive indices of water and air. Because the wavelength decreases by the same factor, the size of the waist should ideally remain the same within the cell. In practice, however, an increase is anticipated because of aberrations caused by the molded glass wall of the cell. Accordingly, the beam waists within the cell are estimated to be $\omega_x \approx 4.8$ μm, $\omega_y \approx 9.6$ μm.[25]

For the SMD experiments, ultradilute solutions of the dyes in triply distilled water (Cabisco Chemicals) are prepared by serial dilution of a stock solution of known concentration made from the solid dry powder. To test for the possibility of contamination in the process of serial dilution, a blank solution is prepared by one's performing the same steps as in the ultradilute solution preparation, but beginning with clean water.

The sample capillary is conveniently loaded with a microliter aliquot of ultradilute sample through the use of a soft plastic pipette (Eppendorf, Microloader). It is then affixed to a tubular holder (supplied by Eppendorf), which is connected to a water-filled manometer for adjusting the sample injection rate. The holder is mounted on a precision translation stage, which is used to lower the tip into the flow cell through the open top. The level of the sheath water flow within the cell is maintained near the top by a balancing of the input and the output volumetric rates. A bottle of water pressurized by helium gas is used to inject water through a 0.2-μm particulate filter (Gelman Sciences, Acrodisc) and through a glass capillary glued at the top of the cell near the corner (see Fig. 4). The bottom of the cell is connected to another manometer for adjusting the output flow rate.

5. Calculations

A. Single or Double Molecules?

Because molecules pass through the probe region at random times, the probability of having m molecules at any given time has a Poisson distribution with

$$P(m) = \overline{m}^m e^{-\overline{m}}/m!, \tag{11}$$

where $\overline{m}$ is the mean number of molecules in the probe region. The fraction of photon bursts that are caused by two molecules passing simultaneously through the probe region is

$$f = P(2)/P(1) = \overline{m}/2. \tag{12}$$

In the simple flow cell, $\overline{m}$ can be calculated as the concentration divided by the probe volume. However, in the new flow cell, $\overline{m}$ depends on both the concentration of the sample solution in the capillary tip and the injection rate. In the experiments, a concentration of $\sim 10^{-13}$ M is used, and the injection rate is gradually increased to give a suitably low value for $\overline{m}$. For an estimated total SMD detection efficiency, e, and the experimentally determined transit time, $2\delta_t$, $\overline{m}$ may be determined from the observed rate of photon bursts, $\overline{M}$, as

$$\overline{m} = \overline{M}\, 2\delta_t/e. \tag{13}$$

Thus, if the observed number of bursts is $\overline{M}$, then the fraction of peaks that are due to two molecules passing through the probe region simultaneously is

$$f = \overline{M}\delta_t/e. \tag{14}$$

B. Signal Strength Estimation

The mean number of fluorescence photons expected when a molecule passes through the laser beam, $\overline{n}_f$, is determined by the number of times the molecule is excited, N, the fluorescence quantum yield of the molecule, Φ_f, and the overall photon detection efficiency of the instrument, E, i.e.,

$$\overline{n}_f = N\Phi_f E. \tag{15}$$

As the molecule passes through the Gaussian profile of the focused laser, the intensity and hence the probability of excitation vary. For a molecule with absorption cross section σ_a, the probability of excitation per laser pulse is

$$p_{\text{excite}}(t) = 1 - \exp[-\sigma_a I(t)/3RE_\gamma], \tag{16}$$

where R is the laser repetition rate and E_γ is the photon energy. The factor of 3 accounts for the random distribution of the dipole moment of the molecule with respect to the polarization of the laser excitation pulse. When excitation is far below saturation, Eq. (16) gives

$$p_{\text{excite}}(t) \approx \sigma_a I(t)/3RE_\gamma, \tag{17}$$

and the number of excitations per unit time is

$$N_{\text{excite}}(t) = \sigma_a I(t)/3E_\gamma. \tag{18}$$

If the molecule passes through the center of the laser beam, $I(t)$ is given by Eq. (4). The total number of laser excitations experienced by a molecule that passes through the center without photodegradation is thus

$$N = \int_{-\infty}^{\infty} N_{\text{excite}}(t)\mathrm{d}t = \sqrt{\frac{2}{\pi}}\,\frac{\sigma_a P\delta_t}{3E_\gamma\omega_x\omega_y}. \tag{19}$$

The values for the various parameters in Eq. (19) used in the experiment of Subsection 6.B. are listed in Table 1. The peak excitation probability per pulse is calculated from the listed parameters to be 0.096, indicating that excitation is well below saturation. Using the parameters listed in the table gives $N = 4220$.

In the lower part of Table 1 are the efficiencies of the various filters and components that contribute to the overall efficiency of photon detection. Also included is an additional 20% loss of signal that is due to the 0.8-μs dead time of the SPAD, calculated by Eq. (2). With the values of N, E, and Φ_f from the table, the mean number of detected fluorescence photons as calculated from Eq. (15) is

$$\overline{n}_f = 14.2. \tag{20}$$

Because of the uncertainty in the efficiencies of the

Table 1. Parameters for S-101 and Experimental Parameters used for Calculations

Parameter	Symbol	Value
Absorption cross section	σ_a	3.7×10^{-16} cm^2
Fluorescence quantum efficiency	Φ_f	0.35
Photodegradation quantum efficiency	Φ_D	5.5×10^{-5}
Laser power	P	14 mW
Photon energy at 585 nm	E_γ	3.4×10^{-19} J
Laser beam waist in flow direction	ω_x	4.8 μm
Laser beam waist in transverse direction	ω_y	9.4 μm
Laser repetition rate	R	7.6×10^7 s^{-1}
Peak excitation probability per pulse	P_{excite}	0.096
Transit time	$2\delta_t$	1.0 ms
Mean number of excitations	N	4220
Collection objective efficiency		0.12
SPAD quantum efficiency		0.55
Throughput due to SPAD dead time		0.80
Throughput of collection objective		0.93
Throughput of spectral filters		0.40
Throughput of remaining optics		0.80
Throughput of time filter		0.60
Overall photon detection efficiency	E	9.6×10^{-3}

various components, the error in the overall detection efficiency and hence in the expected number of fluorescence photons is estimated to be ~25%. Also, the expected signal will be less for molecules that do not pass through the exact center of the laser profile.

C. Background and Photon Statistics

The background is linearly proportional to the laser power and the collection time. In the time interval $2\delta_t$ during which is molecule passes through the beam, the mean number of background photons, $\bar{n}_b$, is given as

$$\bar{n}_b = KP2\delta_t. \tag{21}$$

The empirical proportionality constant, K, accounts for both unrejected Raman scatter from the solvent as well as stray fluorescence. It depends on the number of solvent molecules in the probe volume and on a factor that accounts for the collection and the throughput of the background noise through the various filters. In the experiment of Subsection 6.B, K is found to be $\sim 4.2 \times 10^5\ \mathrm{s}^{-1}\ \mathrm{W}^{-1}$, and for a laser power of 14 mW, the mean number of background counts during an interval of $2\delta_t = 1.0$ ms is ~5.9. Thus, during the transit of a single molecule, the total mean number of detected photons, $\bar{n}$, is expected to be

$$\bar{n} = \bar{n}_f + \bar{n}_b = 14.2 + 5.9 = 20.1. \tag{22}$$

When there are no molecules in the beam, the probability P_0 of having n counts in a time interval $2\delta_t$ is given by the Poisson distribution, i.e.,

$$P_0(n) = \bar{n}_b^n e^{-\bar{n}_b}/n!. \tag{23}$$

For the transit of a single molecule through the center of the laser without photodegradation, the probability is

$$P_1(n) = \bar{n}^n e^{-\bar{n}}/n!. \tag{24}$$

As molecules in the experiment do not necessarily pass through the exact center of the laser beam, the mean number of detected photons, $\bar{n}$, will be smaller. Furthermore, the probability density function $P_1(n)$ will be due to an ensemble average over different trajectories and hence will be broader. However, a well-defined peak in the histogram of burst amplitudes should still be obtainable, provided that most molecules pass close to the center of the probe region. In the case of experiments conducted with the simple flow cell, molecule trajectories that pass near the edges of the probe region will degrade the probability density function so that a well-defined peak is no longer obtained.

D. Photodegradation

The results discussed above apply only to molecules that do not photodegrade. In reality, the probability that a molecule has not photodegraded decreases exponentially with the number of excitations. The mean number of excitations a molecule can endure before photobleaching is the reciprocal of the photodegradation quantum efficiency, Φ_D.

An S-101 molecule in water has $\Phi_d = 5.5 \times 10^{-5}$ and thus can on average be excited 18,180 times before it photodegrades.[26] In the experiment of Subsection 6.B, for a molecule that passes through the center of the laser beam, the mean number of excitations, as given in Table 1, is $N = 4220$. The fraction of molecules that photodegrade before leaving the probe region is therefore $1 - \exp(-N\Phi_D) = 0.207$. This fraction would be decreased for a molecule with a lower photodegradation quantum efficiency such as R6G. Note, however, that in the first experimental demonstration of SMD,[13] R6G was used and almost all molecules photodegraded.

For efficient SMD, the number of excitations should be minimized to reduce the probability of photodegradation. However, even if a molecule photodegrades, it may still have generated enough photons to be detected. Conversely, it is always possible that a molecule may photodegrade the very first time it is excited, before any fluorescence is detected.

6. Experimental Results

A. Simple Flow Cell

To demonstrate that single molecules can be detected at relatively high flow velocities, experiments are first conducted within a simple flow cell. The experimental geometry is the same as that of the later experiments except that the sample molecules are not confined to a narrow stream. Results are shown for a laser power of 12 mW and a concentration of S-101 of $\sim 10^{-14}$ M.

Figure 6 shows a peaked autocorrelation function that is due to S-101 molecules transiting through the laser beam and a flat autocorrelation function that is due to the blank solution. A Gaussian fit to the peak and Eq. (7) give the molecular transit time as $2\delta_t = 1.5$ ms. There is a non-Gaussian feature superimposed near the origin that may possibly be due to photodegradation.

Figure 7 shows a 300-ms segment of the photon

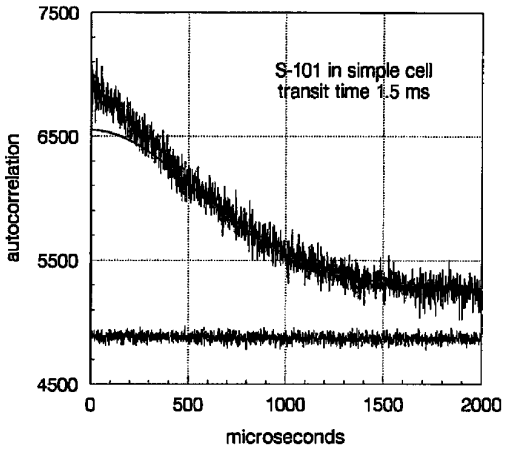

Fig. 6. Autocorrelations from S-101 and water in the simple flow cell.

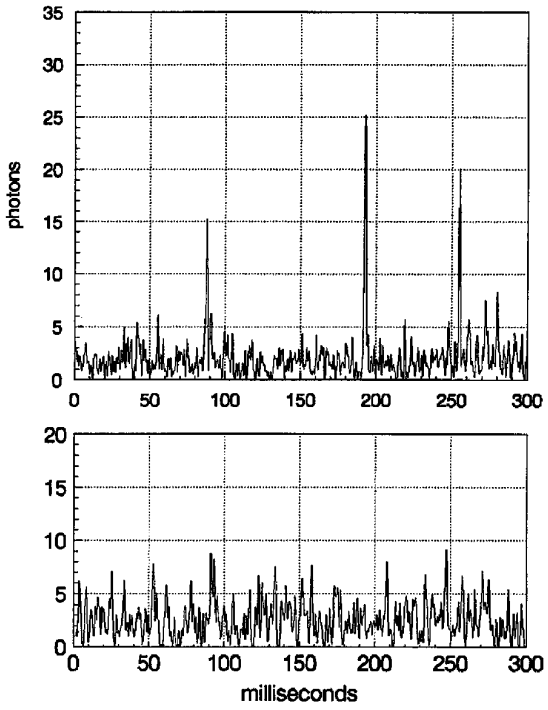

Fig. 7. Photon-burst signals from S-101 and water in the simple flow cell.

burst signal, as calculated by Eq. (9). In this segment of data at least three molecules are detected. In the lower part of the figure is another 300-ms segment of data obtained with clean water. In this case there are no bursts >9.

Figure 8 shows the histograms of photon-burst amplitudes that are due to S-101 molecules and clean water. As molecules are not confined to a narrow stream but completely fill the cell, most molecules do not pass through the probe region. Also, many molecules pass near the edges of the laser beam and give smaller amplitude photon bursts. Thus the distribution that is due to molecules is equal to that of the blank plus a monotonically decreasing component.

B. Capillary Injection System

To obtain a high total detection efficiency, experiments are next conducted with the new sample injection capillary. Figure 9 gives the autocorrelation functions for S-101 molecules and for the blank solution. The blank is obtained when the tip of the sample delivery capillary is translated away from the probe region out of the field of view of the spatial filter. An alternative way to obtain a blank without moving the tip is to stop the molecule delivery by the application of negative pressure at the manometer that is connected to the sample delivery capillary. When S-101 molecules are delivered from the tip, the autocorrelation function exhibits a distinct peak. The mean molecular transit time is determined as $2\delta_t = 1.0$ ms from Eq. (7) and the Gaussian fit to the peak, which is also shown in Fig. 9.

Figure 10 shows 100-ms segments of the photon-burst signals, processed by Eq. (9), from the S-101 sample and from the blank. Bursts that are due to S-101 molecules are clearly above the background noise level. Note that in the top part of the figure there are 13 photon bursts of amplitude ≥11. If a longer period of time is observed, the mean rate of peaks is found to be $\bar{M} \sim 150\ s^{-1}$. From Eq. (14) and the overall detection efficiency of $e = 0.8$ estimated below, the fraction of bursts that are due to two molecules passing simultaneously through the probe volume is $f \sim 9\%$. Thus, in this particular experimental run, on average approximately one in every 11 peaks is due to two molecules, and most probably the second peak, of amplitude ~41 photons, should be counted as two molecules passing simultaneously.

Figure 11 shows the histograms of the photon-burst amplitudes for S-101 molecules and the blank. For the blank, there are no bursts of amplitude >13 and most bursts are <11. The mean burst amplitude is ~6. For the dye molecule sample, there are still bursts of amplitude ~6, but most bursts have an

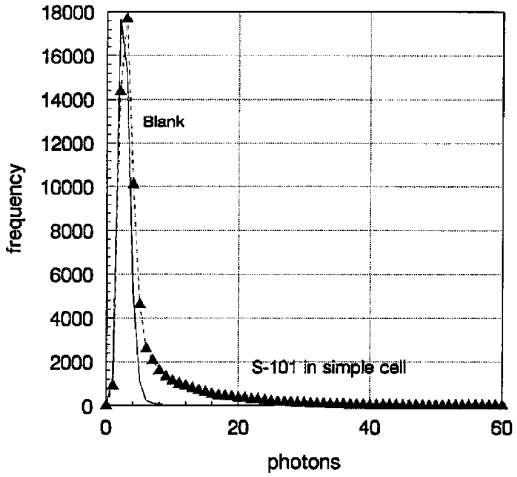

Fig. 8. Histograms of burst amplitudes from S-101 and water in the simple flow cell.

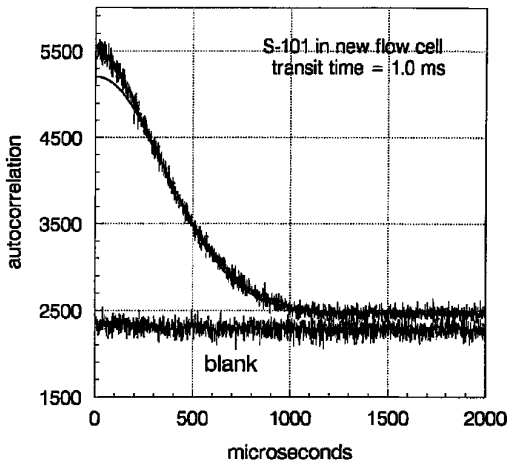

Fig. 9. Autocorrelations from S-101 and blank with the capillary injection system.

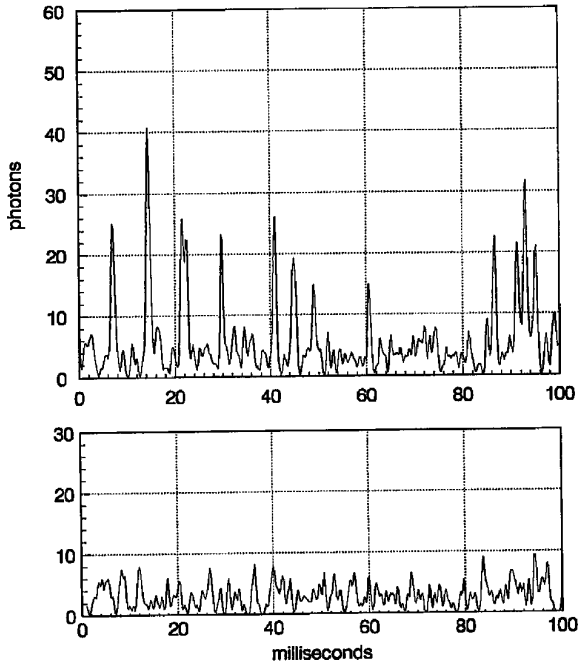

Fig. 10. Photon-burst signals from S-101 and blank with the capillary injection system.

amplitude ≥11. Furthermore, there is a distinct peak in the histogram at an amplitude of 18 photons and a distinct valley at an amplitude of 11. This behavior is substantially different from that of the histogram in Fig. 8 and illustrates that most molecules pass through the central part of the probe region.

For the dye molecule sample, the distribution of burst amplitudes is expected to be due to the sum of a component that is due to background fluctuations and a component that is due to the passage of S-101 molecules. Bursts of amplitude ≥11 are attributed to S-101 molecules whereas bursts of <11 are attributed to random fluctuations in the background. S-101 molecules that generate bursts of <11 are undetected. If the component that is due to molecules only is extrapolated, the fraction of molecules that escape detection is estimated to be ~20%.

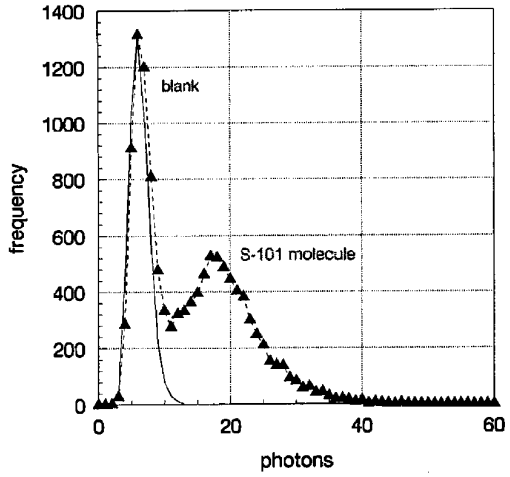

Fig. 11. Histograms of burst amplitudes from S-101 and blank with the capillary injection system.

The mean burst amplitude for molecules that pass through the center of the laser without photodegradation is estimated in Subsection 5.B. and 5.C. to be 20.1. As most molecules are not expected to pass exactly through the center of the laser beam and some molecules photodegrade, resulting in smaller bursts, the distribution is expected to peak at a value of <20.1. Note that the peak of the distribution in Fig. 11 is at 18, in good agreement with the estimate. In Subsection 5.D., the fraction of molecules that photodegrade while passing through the probe volume is calculated to be ~20%, although some molecules that photodegrade are still expected to give enough photons for detection. This value approximately agrees with the estimated 80% detection efficiency. Furthermore, Monte Carlo simulations of the experimental configuration[27] with the parameters from Table 1 give a signal and a histogram of burst amplitudes in agreement with the experiment with the experiment and also predict a detection efficiency of ~80%, with loss that is due largely to photodegradation. However, further experiments to count the total number of molecules in a sample of known volume and concentration are necessary for an independent measurement of the detection efficiency.

7. Conclusions

In all prior experiments to detect single chromophore molecules in aqueous solution, only a small fraction of molecules pass through the laser beam. Previously quoted detection efficiencies do not refer to the total efficiency but only to those molecules that happen to pass through the central probe region. Furthermore, the signal amplitudes from individual molecules vary widely because many molecules pass through the edges of the Gaussian laser profile.

In this work, molecules are introduced into a sheath flow through a fine capillary with a submicrometer opening placed immediately above the tightly focused laser beam. Fast-flow velocities are used to reduce diffusional spreading so that almost all sample molecules pass in a narrow stream through the center of the probe region. SMD within the fast-flow stream is made possible by the use of a high-quantum-efficiency solid-state photon detector, a subnanosecond low dead-time anticoincidence circuit for temporal discrimination of promptly scattered Raman that is due to the solvent, and a critical optical design that includes a high numerical aperture collection objective.

The fluorescent tagging agent S-101, which has a fluorescence yield of only 0.35 and a photostability of 2.9 times less than that of RGG, is detected with a high total efficiency of ~80%, limited mainly by its relatively poor photostability. The experiment demonstrates the detection of individual single chromophore molecules in aqueous solution with transit

times of ~1 ms that are the shortest reported to date. Results are presented demonstrating rapid counting of the single molecules at a rate of ~150 s^{-1}, considerably higher than in all previous experiments. Furthermore, as most molecules experience approximately the same laser excitation and as the probability of photodegradation is relatively low, the histogram of photon burst amplitudes has a distinct peak located clearly above the background fluctuations.

The experimental apparatus should permit future analytical measurements in which a count is made of the number of fluorescently tagged molecules within a small aliquot of ultradilute sample. Also, the quantitative photon burst signal obtained from each molecule should permit molecular species of different brightness to be distinguished.

This research was supported by a grant from the Whitaker Foundation.

Note added in proof: Efficient SMD within an 11-μm capillary has recently been demonstrated with the infrared dye IR140 in methanol solution.[28]

References and Notes

1. E. Betzig, "High-density near-field optical recording," in *OSA Annual Meeting,* Vol. 16 of 1993 OSA Technical Digest Series (Optical Society of America, Washington, D.C., 1993), p. 78.
2. L. M. Davis, F. R. Fairfield, M. L. Hammond, C. A. Hager, J. H. Jett, R. A. Keller, J. H. Halm, L. A. Krakowski, B. Marrone, J. C. Martin, H. L. Nutter, R. R. Ratliff, E. B. Shera, D. J. Simpson, S. A. Soper, and C. W. Wilkerson, "Rapid sequencing of DNA based on single molecule detection," Los Alamos Sci. **20,** 280–285 (1992).
3. M. Eigen and R. Rigier, "Sorting single molecules: Application to diagnostics and evolutionary biotechnology," Proc. Natl. Acad. Sci. USA **91,** 5740–5747 (1994).
4. J. Suijlen and W. van Leussen, "Recent developments in large-scale tracing by fluorescent tracers," in *Esturine Water Quality Management,* W. Michaelis, ed. (Springer-Verlag, New York, 1990), pp. 181–196.
5. S. D. Lidofsky, W. D. Hinsberg III, and R. N. Zare, "Enzyme-linked sandwich immunoassay for insulin using laser fluorometric detection," Proc. Natl. Acad. Sci. USA **78,** 1901–1905 (1981).
6. Y. F. Cheng, S. Wu, D. Y. Chen, and N. J. Dovichi, "Interaction of capillary zone electrophoresis with a sheath flow cuvette detector," Anal. Chem. **62,** 496–503 (1990).
7. W. E. Moerner and T. Basché, "Optical spectroscopy of single impurity molecules in solids," Angew. Chem. Int. Ed. Engl. **32,** 457–476 (1993), and references therein.
8. E. Betzig and R. J. Chichester, "Single molecules observed by near-field scanning optical microscopy," Science **262,** 1422–1425 (1993).
9. X. S. Xie and R. C. Dunn, "Probing single molecule dynamics," Science **265,** 361–364 (1994).
10. W. P. Ambrose, P. M. Goodwin, J. C. Martin, and R. A. Keller, "Alterations of single molecule fluorescence lifetimes in near-field optical microscopy," Science **265,** 364–367 (1994).
11. M. Ishikawa, K. Hirono, T. Hayakawa, S. Hosoi, and S. Brenner, "Single-molecule detection by laser-induced fluorescence technique with a position-sensitive photon-counting apparatus," Jpn. J. Appl. Phys. **33,** 1571–1576 (1994).
12. M. D. Barnes, K. C. Ng, W. B. Whitten, and J. M. Ramsey, "Detection of single rhodamine 6G molecules in levitated microdroplets," Anal. Chem. **65,** 2360–2365 (1993).
13. E. B. Shera, N. K. Seitzinger, L. M. Davis, R. A. Keller, and S. A. Soper, "Detection of single fluorescent molecules," Chem. Phys. Lett. **174,** 553–557 (1990).
14. S. A. Soper, L. M. Davis, and E. B. Shera, "Detection and identification of single molecules in solution," J. Opt. Soc. Am. B. **9,** 1761–1769 (1992).
15. S. A. Soper, Q. L. Mattingly, and P. Vegunta, "Photon burst detection of single near-infrared fluorescent molecules," Anal. Chem. **65,** 740–747 (1993).
16. C. W. Wilkerson, P. M. Goodwin, W. P. Ambrose, J. C. Martin, and R. A. Keller, "Detection and lifetime measurement of single molecules in flowing streams by laser-induced fluorescence," Appl. Phys. Lett. **62,** 2030–2032 (1993).
17. L. Q. Li and L. M. Davis, "Single photon avalanche diode for single molecule detection," Rev. Sci. Instrum. **64,** 1524–1529 (1993).
18. L. Q. Li, "Single molecule detection in solution," Ph.D. dissertation (University of Tennessee, Space Institute, Tullahoma, Tennessee, 1994).
19. D. C. Nguyen and R. A. Keller, "Detection of single molecules of phycoerythrin in hydrodynamically focused flows by laser-induced fluorescence," Anal. Chem. **59,** 2158–2161 (1987).
20. A. Castro, F. R. Fairfield, and E. B. Shera, "Fluorescence detection and size measurement of single DNA molecules," Anal. Chem. **65,** 849–852 (1993).
21. P. M. Goodwin, M. E. Johnson, J. C. Martin, W. P. Ambrose, B. L. Marrone, J. H. Jett, and R. A. Keller, "Rapid sizing of individual fluorescently stained DNA fragments by flow cytometry," Nucl. Acids Res. **21,** 803–806 (1993).
22. L. M. Davis and L. Q. Li, "Ultrasensitive sub-nanosecond time-gated detection using a single photon avalanche diode," in *Applications of Photonic Technology,* G. A. Lampropoulos, ed. (Plenum, New York, 1994).
23. G. R. Haugen, B. W. Wallin, and F. E. Lytle, "Optimization of data-acquisition rates in time-correlated single-photon fluorimetry," Rev. Sci. Instrum. **50,** 64–72 (1979).
24. K. Peck and L. Stryer, A. N. Glazer, and R. A. Mathies, "Single-molecule fluorescence detection: autocorrelation criterion and experimental realization with phycoerythrin," Proc. Natl. Acad. Sci. USA **86,** 4087–4091 (1989).
25. The estimate is consistent with an approximate measurement obtained by one's viewing the light scatter as the capillary tip is scanned through the waist.
26. S. A. Soper, E. B. Shera, L. M. Davis, H. L. Nutter, and R. A. Keller, "The photophysical constants of several fluorescent dyes pertaining to ultrasensitive fluorescence spectroscopy," Photochem. Photobiol. **57,** 972–977 (1993).
27. L. M. Davis and L. Q. Li, "Monte Carlo model of a single molecule counting experiment," in *Laser Applications of Chemical Analysis,* Vol. 5 of 1994 OSA Technical Digest Series (Optical Society of America, Washington, DC., 1994), pp. 206–209.
28. Y. H. Lee, R. G. Maus, B. W. Smith, and J. D. Winefordner, "Laser-induced flourescence detection of a single molecule in a capillary," Anal. Chem. **66,** 4142–4149 (1994).